The definitive version of this article is available at http://ieeexplore.ieee.org

Published as: Medeiros, C.R.; Lima, E.B.; Costa, J.R.; Fernandes, C.A., "Wideband Slot Antenna for WLAN Access Points," *Antennas and Wireless Propagation Letters, IEEE* , vol.9, no., pp.79-82, 2010 Doi: http://dx.doi.org/10.1109/LAWP.2010.2043332

Wideband Slot Antenna for WLAN Access Points

Carla R. Medeiros, Eduardo B. Lima, Jorge R. Costa, *Senior Member, IEEE*, and Carlos A. Fernandes, *Senior Member, IEEE*

***Abstract*—This letter presents a new printed slot antenna with cavity back for wireless local area network (WLAN) access points (base stations) providing wideband operation bandwidth at least from 2.5 to 4.8 GHz. The design is based upon an ultrawideband (UWB) antenna configuration modified with the inclusion of a cavity back in order to produce stable unidirectional radiation pattern. The new configuration also ensures a stable linear polarization with cross-polarization level below −20 dB. Results are confirmed with measurements. Not disregarding other applications, the new design is especially adequate for multiple-input–multiple-output (MIMO) space and polarization diversity arrangements, presenting low cross polarization and very low coupling to adjacent elements.**

***Index Terms*—Cavity back, printed wideband antenna, tapered slot antenna, wireless local area network (WLAN).**

I. Introduction

WIDEBAND antennas are one attractive approach to provide user access to a number of existing and emerging wireless personal communication standards covering a wide frequency spectrum. For indoor access points (APs), it is sometimes required that the antenna radiation pattern is unidirectional to allow mounting it against a wall or surface. Desirably, the antenna should also be compact and low profile.

Next-generation standards (LTE and WiMAX) are most likely to use multiple-input–multiple-output (MIMO) technology to improve system reliability and/or data throughput [1], [2]. However, in order to maximize MIMO performance, the channel link between each transmitter and receiver antenna pair must be statistically independent [3]. Mutual coupling between elements of the antenna array increases correlation between channels, reducing system capacity [4]. Poor diversity in the propagation multipath also deteriorates MIMO performance. However, the use of arrays with polarization diversity can improve channel independence when the multipath fading is only partially correlated [5]. Therefore, further to low coupling between adjacent antenna elements, a MIMO antenna should also present a pure and frequency stable polarization.

This letter proposes an antenna that can be used as a MIMO array element verifying the previously referred requirements related to bandwidth, polarization, and coupling, but it focuses only on the antenna element design and characterization. The MIMO array and its impact on MIMO performance are out of the scope and will appear elsewhere.

Different wideband antenna configurations are well known [6], however only some of these present unidirectional radiation patterns. It is the case of wideband antennas incorporating a ground plane like monopoles, patch antennas [7], [8], or dielectric resonators [9]. Patch antennas are usually low-profile, yet techniques used to enhance their bandwidth tend to drastically deteriorate polarization purity (when slots are used) or increase mutual coupling with respect to adjacent array elements (when substrate thickness is increased) [7], [8].

A different approach to achieve the required specifications is to use a bidirectional wideband antenna and introduce a back surface to force unidirectional radiation. Electronic band-gap (EBG) surfaces may be used to obtain shallow structures, but they are usually frequency-selective, compromising the overall antenna bandwidth: In [10], a wideband dipole was placed close to an EBG achieving 55% bandwidth, but with a very frequency dependent radiation pattern.

Alternatively, a cavity back can be used. One of the most common examples is the cavity-backed spiral antenna [11], which exhibits very large bandwidth (at least 100%) and stable circular polarization. The overall diameter of the cavity is usually larger than $0.8\lambda_{inf}$ (lower frequency wavelength). Many other wideband antenna configurations have been used with a cavity back [12], but the overall size is at best larger than $0.75\lambda_{inf}$.

No antenna appears to be reported that is simultaneously wideband with a frequency-stable unidirectional radiation pattern and low cross polarization and that allows very close packing to form a compact array with low mutual coupling. In [13] and [14], the authors have proposed a new crossed exponentially tapered slot antenna (XETS) for ultrawideband (UWB) systems with 110% impedance bandwidth. That compact $(0.36\lambda_{\text{inf}} \times 0.36\lambda_{\text{inf}})$ configuration had a very stable polarization, low cross-polarization level over the entire bandwidth, and very low coupling to adjacent elements in very packed arrays [13]. However, that design of the XETS exhibited a bidirectional radiation pattern. Therefore, the present letter presents a modification of the XETS design and configuration that incorporates a mesh cavity back to produce unidirectional radiation pattern. Onward, we will refer this configuration as the CXETS.

Manuscript received January 06, 2010. First published February 17, 2010; current version published nulldate. This work was supported by the European Union under Project FP7 ICT-2007-216715 (NewCom++).

C. R. Medeiros, E. B. Lima, and C. A. Fernandes are with the Instituto de Telecomunicações, IST, 1049-001 Lisboa, Portugal (e-mail: Carla.Medeiros@lx.it.pt; Eduardo.Lima@lx.it.pt; Carlos.Fernandes@lx.it.pt).

J. R. Costa is with Instituto de Telecomunicações, IST, 1049-001 Lisboa, Portugal, and also with ISCTE-Lisbon University Institute, 1649-026 Lisboa, Portugal (e-mail: Jorge.Costa@lx.it.pt).

Color versions of one or more of the figures in this letter are available online at http://ieeexplore.ieee.org.

Digital Object Identifier 10.1109/LAWP.2010.2043332

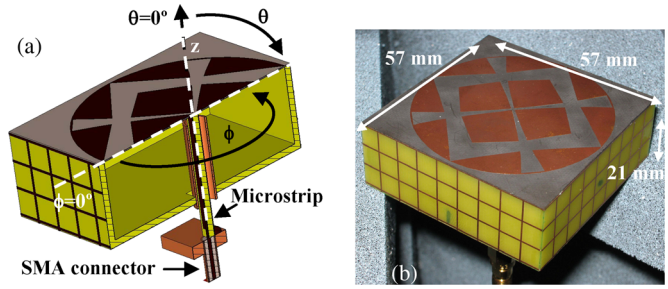

Fig. 1. (a) Cut along the E-plane of the CST antenna model. (b) Photograph of the prototype.

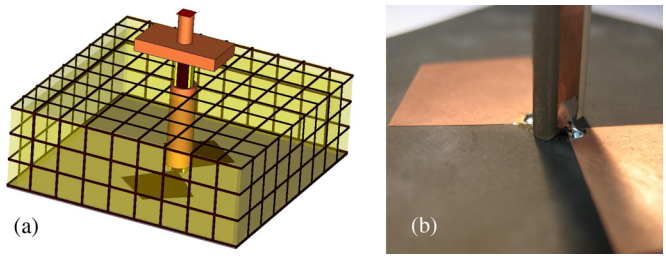

Fig. 2. (a) Bottom face of the XETS DUROID substrate with the feeding petals seen through transparent mesh cavity. (b) Photograph of the feeding microstrip line and the XETS back petals.

II. Antenna Description

The new antenna configuration is shown in Fig. 1(a). The radiating element is based on a crossed exponentially tapered slot (XETS) configuration with an intersecting square slot. The reasoning for this configuration was explained for the bidirectional antenna by the authors in [13] and [14]. A parallelepiped cavity is used in this letter instead of the more common cylindrical one to enable closer packing of side-by-side CXETS when forming a compact array, taking advantage of the very low mutual coupling. The introduction of the cavity to reduce back-radiation actually increases the quality factor of the antenna with consequent reduction of its bandwidth. In many reported cases, the quality factor is intentionally lowered by partly loading the cavity edges with absorbers [11]. This tends to reduce the radiation efficiency over part or all of the operating bandwidth. Alternatively, in the present configuration, the metallic cavity walls are replaced by a squared metallic mesh printed on FR4 substrate. By adjusting the mesh size and cavity depth, a compromise can be found between impedance bandwidth and back-radiation level.

The proposed CXETS was designed to operate across the 2.5–4.8-GHz frequency interval. It covers WiMax 802.16 (2.5–2.7 GHz, USA), LTE (2.5–2.7 GHz, Europe), WiMax 802.16 (3.4–3.6 GHz, worldwide), WiFi 802.11y (3.6–3.7 GHz, USA), and the lower spectrum of UWB (3.1–4.8 GHz, USA). CST Microwave Studio transient solver [15] was used to explore the CXETS configuration. The XETS element was optimized mainly in terms of bandwidth and radiation pattern, while the cavity dimensions and mesh size were optimized to obtain better than 10 dB front-to-back ratio (f/b). Of course the CXETS was designed and optimized as a whole structure. The simulation model is shown in Fig. 1(a).

As before, the XETS element is printed on DUROID 5880 substrate with permittivity $\varepsilon_r = 2.2$, loss tangent $\tan(\delta) = 0.0009$, and thickness $h_{5880} = 10$ mil $= 0.254$ mm. Cavity mesh walls are printed on FR4 substrate, $\varepsilon_r = 4.9$, $\tan(\delta) = 0.025$, and thickness $h_{\mathrm{FR4}} = 1.6$ mm. The inner volume of the cavity is filled with low-density styrofoam ($\varepsilon_r \approx 1.05$) just to provide physical support to the supple 10-mil DUROID substrate.

Two opposing petals on the XETS front face are replicated at the bottom face of the DUROID substrate, which are used to feed the antenna (see Fig. 2). These back petals couple capacitively at RF with the corresponding front petals of the antenna. CXETS is a balanced antenna, intended for use with a differential topology IC transceiver (or mixer) mounted directly at these feeding points [16]. Since the integration of such ICs is out of the scope of the letter, a dedicated wideband feed line is used for antenna test purposes. A quasi-microstrip line is soldered between these back petals, defining the antenna E-plane ($\phi = 0°$). It is printed on FR4 substrate, with thickness $h_{\mathrm{FR4}} = 1.6$ mm; strip width is 2.8 mm, and ground plane width is 4 mm (which is not very different from the strip width). The ground plane is soldered at one of the back petals, while the strip is soldered at the opposite petal. This microstrip line ends on a SMA connector [Fig. 2(a)]. A hollow cylinder brass tube (with 5 mm inner diameter and 6 mm outer diameter) envelops the microstrip line inside the cavity to isolate the feeding line from the cavity inner fields. The tube does not touch the CXETS back petals nor the microstrip, but it extends slightly out the cavity without touching the mesh. The equivalent line impedance of the enveloped microstrip is 50 Ω.

TABLE I
Antenna Parameter Values in Millimeters

D_s	L_{out}	L_{in}	w_s	L	w_0	C_0
54	35.7	27.9	9	53	0.72	12.7

The best set of parameter values found after antenna optimization is indicated in Table I (the same parameter naming is used as in [13]).

The overall antenna dimensions [Fig. 1(b)] are $57 \times 57 \times 21$ mm^3 $(0.48\lambda_{\mathrm{inf}} \times 0.48\lambda_{\mathrm{inf}} \times 0.18\lambda_{\mathrm{inf}})$, where λ_{inf} is the wavelength at the lower operating frequency of 2.5 GHz. Due to the presence of the cavity, the redesigned XETS element is slightly larger than the $0.36\lambda_{\mathrm{inf}}$ bidirectional XETS developed for UWB [13], [14]. The optimum square mesh size (considering the required f/b) was found to be 6 mm.

Fig. 1 shows that the edge of the XETS metallization reaches almost the inner border of the FR4 box. Therefore, when placing two antennas adjacent to each other to form an array, the smallest separation between adjacent XETS metallization will be only 3 mm $(0.025\lambda_{\mathrm{inf}})$.

III. Measured Performance

The magnitude of the measured input reflection coefficient is shown in Fig. 3, superimposed on CST simulations for the structure with the presented microstrip line feed and alternatively with a discrete port feed (balanced feed) topped with a 1-cm^2 transceiver chip. Measured results show an overall similarity to the corresponding CST prediction. The operating band-

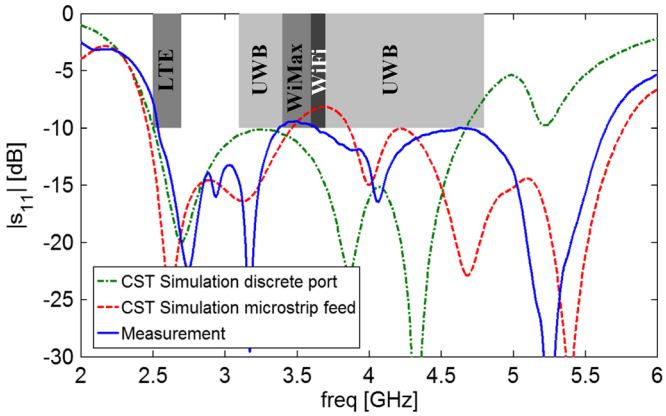

Fig. 3. Measured and simulated amplitude of the antenna input reflection coefficient.

width extends from 2.5 up to 5.5 GHz, however, for the balanced transceiver case, which is closer to the end application; the upper limit is 4.8 GHz, covering the bands assigned to several wireless standards marked on Fig. 3.

The magnitude of the measured radiation pattern is presented in Fig. 4 for three different frequencies within the operating bandwidth. The ordinate is normalized to the maximum value. Cross polarization in the E-plane ($\phi = 0°$) is at least 20 dB below the copolarization level. Measured front-to-back ratio (f/b) ranges between 11 and 20 dB within the operating bandwidth.

Fig. 5 presents measured gain versus frequency. It increases with frequency from 5.5 to 8 dBi. Gain transition near 4 GHz relates to the narrowing of the main beam beyond this point. Fig. 5 also shows the simulated total radiation efficiency, which is always above 80% within the desired bandwidth of operation. Efficiency values measured at discrete frequencies are superimposed (crosses in Fig. 5), obtained using different resonant Wheeler cap cavities [17]. The results agree reasonably with simulation.

Fig. 6 shows the simulated near-field distribution (E-field) along the H-plane ($\phi = 90°$) for frequencies near the edges of the desired operation band. It is noticed that the cavity lateral walls greatly reduce the magnitude of the side radiated fields. Although this lateral blockage is not so drastic in the E-plane, preliminary simulations have shown that when packing side-by-side CXETS in orthogonal polarization arrangement to form a compact MIMO array, mutual coupling level stays below -25 dB at the lower frequency. As previously mentioned, MIMO CXETS array and its impact on MIMO performance are out of the scope of the present letter and will appear elsewhere. A similar result concerning coupling was obtained by simulation and measurement for the UWB bidirectional XETS design [13], [14].

IV. Conclusion

A new antenna configuration, CXETS, is reported, which is simultaneously wideband with frequency-stable unidirectional radiation pattern, low cross polarization, and high front-to-back ratio and which allows very close packing to form a compact array with low mutual coupling, making it a perfect

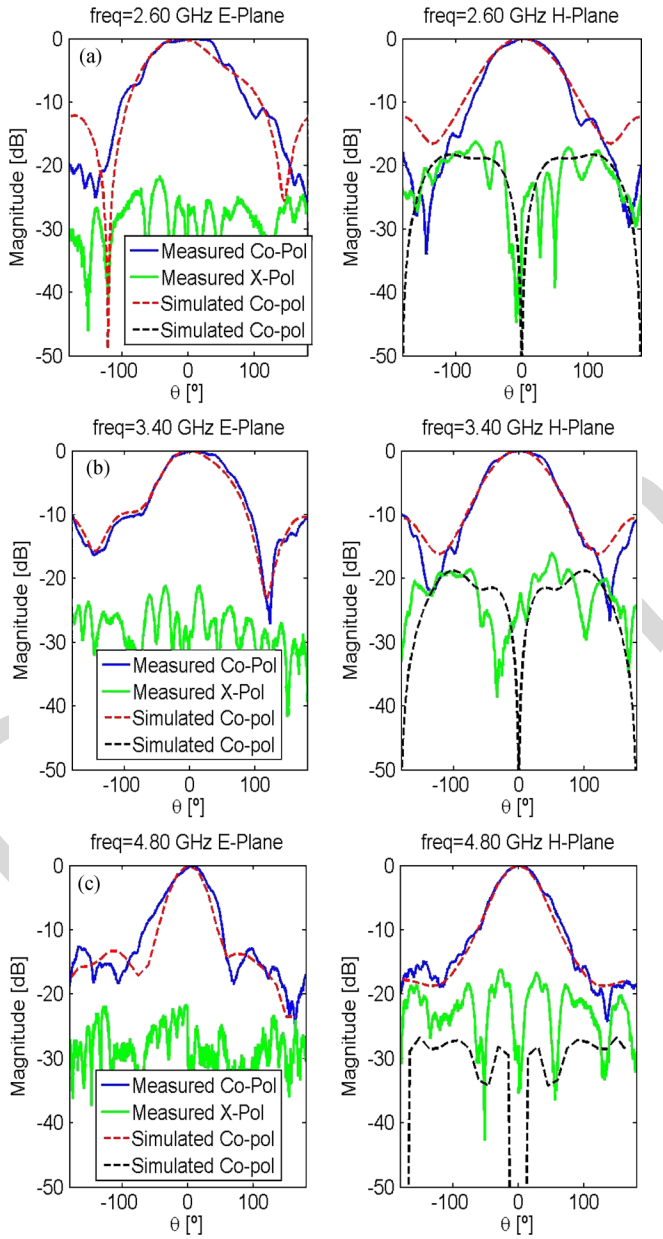

Fig. 4. Measured and simulated radiation pattern for (a) 2.6, (b) 3.4, and (c) 4.8 GHz.

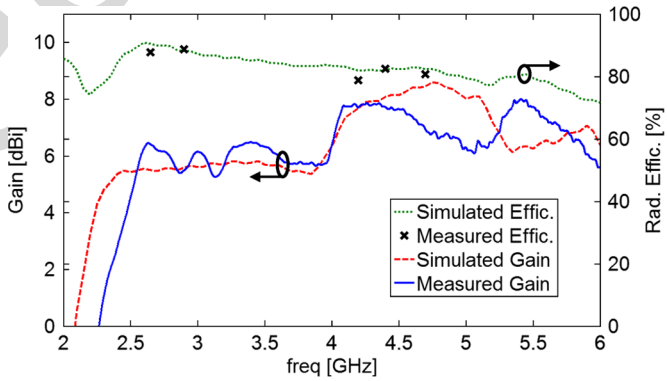

Fig. 5. Measured and simulated gain and simulated radiation efficiency along the antenna bandwidth.

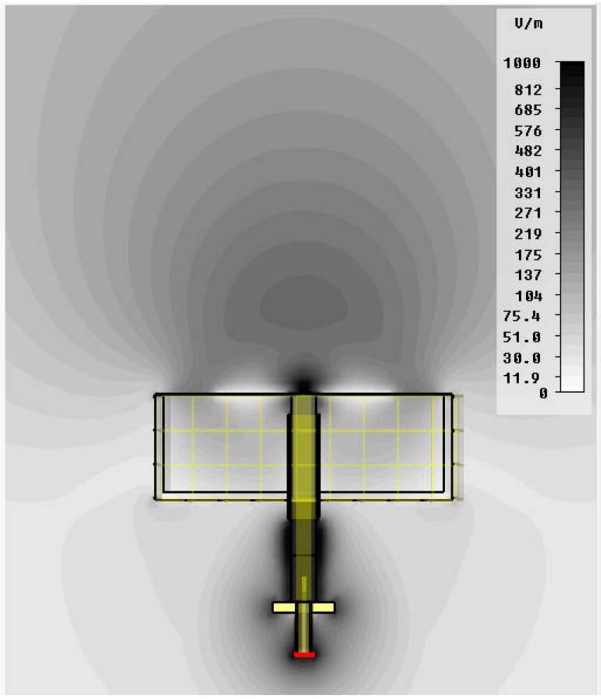

(a)

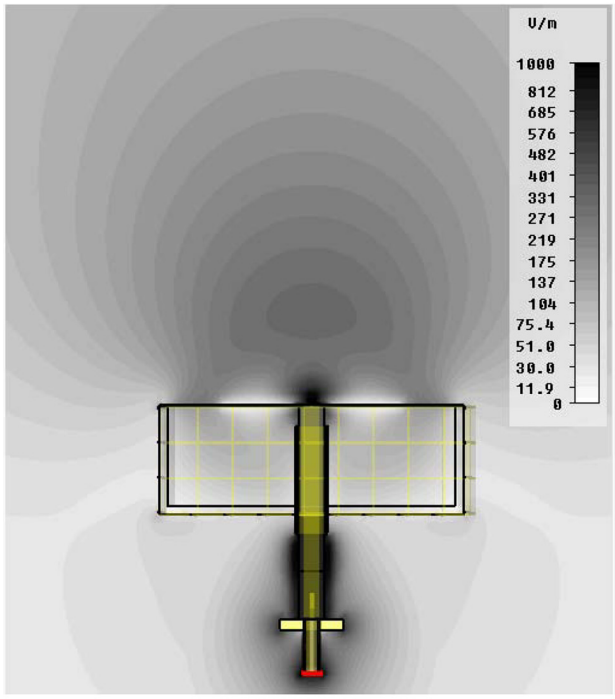

(b)

Fig. 6. CST simulation for the amplitude of the near-field distribution along the H-plane ($\phi = 90°$) at the frequency using discrete quasi-microstrip line feed: (a) 2.6 and (b) 4.8 GHz.

candidate for indoor access points exploring MIMO spatial and polarization diversity. A single antenna was analyzed and shown to cover several wireless communication services within the 2.5–4.8-GHz frequency interval. It is a slot-based antenna with a low-profile mesh cavity back. Overall size is $57 \times 57 \times 21$ mm^3, corresponding to $0.48 \times 0.48 \times 0.18$ of the lower frequency wavelength. Although this balanced antenna is intended for using differential topology transceivers mounted directly at the antenna feeding points, a dedicated wideband feed line was designed only for antenna test purposes. A prototype was fabricated, and the antenna performance was confirmed experimentally. The radiation pattern is stable across the bandwidth, with gain ranging from 5.5 to 8 dBi, front-to-back ratio better than 11 dB, stable linear polarization, and cross-polarization level lower than -20 dB. Simulations and measurements show that the radiation efficiency is better than 80% within the bandwidth. The antenna configuration was kept simple, where the XETS antenna element and the cavity walls can be fabricated using printed circuit technology.

ACKNOWLEDGMENT

The authors acknowledge the collaboration from V. Fred and C. Brito for prototype construction and A. Almeida for prototype measurements.

REFERENCES

[1] *Amendment to Air Interface for Fixed and Mobile Broadband Wireless Access Systems—Physical and Medium Access Control Layers for Combined Fixed and Mobile Operation in Licensed Bands*, IEEE Std. 802.16e-2005, 2005.

[2] "3GPP-LTE," August 2009 [Online]. Available: http://www.3gpp.org/article/lte

[3] G. Foschini and M. Gans, "On limits of wireless communications in a fading environment when using multiple antennas," *Wireless Pers. Commun.*, vol. 6, pp. 311–335, 1998.

[4] D. Browne, M. Manteghi, M. Fitz, and Y. Rahmat-Samii, "Experiments with compact antenna arrays for MIMO radio communications," *IEEE Trans. Antennas Propag.*, vol. 54, no. 11, pp. 3239–3250, Nov. 2006.

[5] J. Valenzuela-Valdés, M. García-Fernández, A. Martínez-González, and D. Sánchez-Hernández, "The role of polarization diversity for MIMO systems under Rayleigh-fading environments," *IEEE Antennas Wireless Propag. Lett.*, vol. 5, pp. 534–536, 2006.

[6] *Modern Antenna Handbook*, C. Balanis, Ed. Hoboken, NJ: Wiley, 2008.

[7] V. Sarin, N. Nassar, V. Deepu, C. Aanandan, P. Mohanan, and K. Vasudevan, "Wideband printed microstrip antenna for wireless communications," *IEEE Antennas Wireless Propag. Lett.*, vol. 8, pp. 779–781, 2009.

[8] M. Abbaspour and H. Hassani, "Wideband planar patch antenna array on cylindrical surface," *IEEE Antennas Wireless Propag. Lett.*, vol. 8, pp. 394–397, 2009.

[9] X. Liang, T. Denidni, and L. Zhang, "Wideband L-shaped dielectric resonator antenna with a conformal inverted-trapezoidal patch feed," *IEEE Trans. Antennas Propag.*, vol. 57, no. 1, pp. 271–274, Jan. 2009.

[10] L. Akhoondzadeh-Asl, D. Kern, P. Hall, and D. Werner, "Wideband dipoles on electromagnetic bandgap ground planes," *IEEE Trans. Antennas Propag.*, vol. 55, no. 9, pp. 2426–2434, Sep. 2007.

[11] H. Nakano, T. Igarashi, H. Oyanagi, Y. Iitsuka, and J. Yamauchi, "Unbalanced-mode spiral antenna backed by an extremely shallow cavity," *IEEE Trans. Antennas Propag.*, vol. 57, no. 6, pp. 1625–1633, Jun. 2009.

[12] S. Qu, J. Li, Q. Xue, C. Chan, and S. Li, "Wideband and unidirectional cavity-backed folded triangular bowtie antenna," *IEEE Trans. Antennas Propag.*, vol. 57, no. 4, pp. 1259–1263, Apr. 2009.

[13] J. Costa, C. Medeiros, and C. Fernandes, "Performance of a crossed exponentially tapered slot antenna for UWB systems," *IEEE Trans. Antennas Propag.*, vol. 57, no. 5, pp. 1345–1352, May 2009.

[14] C. Medeiros, J. Costa, and C. Fernandes, "Compact tapered slot UWB antenna with WLAN band rejection," *IEEE Antennas Wireless Propag. Lett.*, vol. 8, pp. 661–664, 2009.

[15] "CST—Computer Simulation Technology," August 2009 [Online]. Available: http://www.cst.com/

[16] P. Datta, X. Fan, and G. Fischer, "A transceiver front-end for ultrawideband applications," *IEEE Trans. Circuits Syst. II, Exp. Briefs*, vol. 54, no. 4, pp. 362–366, Apr. 2007.

[17] M. Geissler *et al.*, "An improved method for measuring the radiation efficiency of mobile devices," in *Proc. IEEE Antennas Propag. Soc. Int. Symp.*, Columbus, OH, Jun. 2003, vol. 4, pp. 743–746.